

Journal of Materials Chemistry A

Accepted Manuscript



This is an *Accepted Manuscript*, which has been through the Royal Society of Chemistry peer review process and has been accepted for publication.

Accepted Manuscripts are published online shortly after acceptance, before technical editing, formatting and proof reading. Using this free service, authors can make their results available to the community, in citable form, before we publish the edited article. We will replace this *Accepted Manuscript* with the edited and formatted *Advance Article* as soon as it is available.

You can find more information about *Accepted Manuscripts* in the [Information for Authors](#).

Please note that technical editing may introduce minor changes to the text and/or graphics, which may alter content. The journal's standard [Terms & Conditions](#) and the [Ethical guidelines](#) still apply. In no event shall the Royal Society of Chemistry be held responsible for any errors or omissions in this *Accepted Manuscript* or any consequences arising from the use of any information it contains.

Hollow carbon nanofiber as stabilizer for in-situ TiO₂/VO₂ co-impregnation with high rate performance and ultra-long cycling life as lithium-ion battery anode

Cite this: DOI: 10.1039/x0xx00000x

Received 00th January 2012,
Accepted 00th January 2012

DOI: 10.1039/x0xx00000x

www.rsc.org/

Xinran Wang^{ab}, Shili Zheng^a, Yi Zhang^a, and Hao Du^{a*}

TiO₂ and VO₂ were first co-impregnated in the shell of electrospun hollow carbon nanofibers. The hierarchical porous structure enabled fast electron transfer and electrolyte penetration, resulting in high power rate and ultra-long cycling life, which makes the structure a promising anode for lithium ion batteries.

Introduction

Owing to its large energy density, lithium ion batteries (LIBs) has been studied for decades to satisfy the rapidly increasing demand of power sources.¹⁻⁴ Recently, the increasing concerns upon unsafe lithium dendrite have promoted the investigation on alternating conventional carbon anode with electrochemically safe material.⁵⁻⁷ Titanium oxide, such as monoclinic TiO₂ and anatase TiO₂, have been attracted much attention because of their large theoretical capacity (~335 mAh g⁻¹), low volume expansion (< 3 %), superb pseudocapacitor-like behaviour and environmental friendliness.⁸⁻¹³ Unfortunately, the low electrical conductivity (10⁻¹³~10⁻¹⁷ S cm⁻¹) constitutes the major obstacle for its application in LIBs in the form of insufficient rate performance and low lithium ion insertion kinetics. To circumvent such drawback, nanostructured TiO₂ has been intensively investigated and proved to be effective on improving the lithium ion diffusion kinetics. However, due to the low thermodynamic stability of nanoparticles, self-aggregation of these nanoparticles occurs upon deep cycling. And the aggregation problem is further accompanied with undesirable isolation between TiO₂ and the conducting agency, leading to poor cycling performance and insufficient power rate.

Bottom-up synthesis of hierarchical TiO₂/carbon composite offers a promising procedure to prevent particle aggregation. In this regard, the recent upsurge emphasized surface modification/functionalization techniques, by which TiO₂ nanoparticles or thin layers are decorated on the exterior of carbon material. Numerous approaches, including sol-gel synthesis, chemical vapour deposition (CVD), atomic layer deposition (ALD), layer-by-layer adsorption and electrospinning technique, have been applied and however, the rate performance of the state-of-the-art structure is still not as sufficient as desire.¹⁴⁻¹⁷ More recently, Liu *et al.* set a very good example on modifying the surface of CNFs through electrospinning and hydrothermal method.¹⁸ A uniform thin layer of TiO₂ nanosheets tightly grew on the interface of the carbon nanofibers (CNFs). Benefitting from the morphology manipulation, the structure made a significant progress in the

perspective of higher power rate and better cycling performance.¹⁸ Unfortunately, their attempt to further increase the weight fraction of TiO₂ nanosheet to about 25 % turns out to be unsuccessful. Highly challenging efforts are required to upgrade the overall energy density by increasing the TiO₂ loading or further re-designing of alternative structure with equally high performance.

In terms of carbon substrate, electrospun hollow carbon nanofiber (HCNFs) is a desirable organization for particle impregnation because of its hierarchical porous architecture. Three types of pores are involved including: the hollow cavity inside the fibre, the nanometer-scaled holes across the fibre and the micrometer-scaled holes between fibres. By introducing HCNFs as the substrate of TiO₂, the current surface modification strategy seems inapplicable to HCNFs because the problem of limited TiO₂ loading can be predicted. Based on the consideration aforementioned, we designed an original structure of particle-impregnated HCNF to increase the conductivity of TiO₂ as well as power rate. TiO₂/VO₂ has been first co-impregnated into HCNFs through the simultaneous coaxial electrospinning techniques. Over 60 (wt. %) of TiO₂ (with 6 % VO₂) was for the first time dispersed and in-situ grown in the carbon shell of HCNFs. As an anode for LIBs, the structure delivered a remarkable capacity of 1016 and 554 mAh.g⁻¹ with potential range of 0-3V and 1-3V (*vs.* Li⁺/Li), respectively. Furthermore, ultra-long cycling performance with narrow potential range was carried out and found to be most stable with reversible capacity of 139 and 90 mAh.g⁻¹ under 15 C and 20 C after 1000 cycles. Although the TiO₂ and VO₂ was deeply immobilized inside the carbon, the hierarchical porous structure enables an even faster lithium ion diffusion than that of TiO₂ particles (7 nm in diameter) suggested by the evaluations on their electrochemical properties.

Results and discussion

The procedure involved in this study is modified from our previous work (see experimental details in ESI†). The solution containing titanium precursor, vanadium precursor and PVP were utilized as the shell solution while the liquid paraffin as the core solution. These two immiscible solutions were directly electrospun

C

Journal Name

into core/shell nanofibers with the appearance of membrane (22×11 cm) in Fig. 1a. With the thermal pyrolysis and oxidation of precursors, a large area of self-standing membrane appeared, as illustrated in Fig. 1b. The membrane was flexible enough to be consequently cut into discs without adding any additives (Fig. 1b inset). SEM image (Fig. 1c) on its interfacial morphology suggested a uniform nanofiber texture (~200 nm in diameter for single fibre) in particular with the micrometer-scale pores derived from the fibre interconnection. The hollow characteristic of the fibre was verified by the cut-edge SEM image in Fig. 1d and the TEM images in Fig. 1e. Clear boundary between the carbon shell (50 nm in thickness) and hollow core (approximately 100 nm in diameter) was observed without any obvious particle formation, an indicative of exceptional TiO₂ and VO₂ dispersion. The SAED pattern (Figure 1e inset) demonstrated the crystallographic property of polycrystalline of these metal oxides. HRTEM image in Figure 1f suggested the formation of relatively small particles with the diameter evaluated to be ~10 nm. It has to be pointed out that because these metal oxides were impregnated into the carbon shell, the diameter was thus estimated by the circle lattice fringe of regionally-crystallized carbon surrounding the particles. Meanwhile, typical mesopores inside the carbon shell of nanofiber was observed, which may form through the removal of solvent and the decomposition of organic precursors. Therefore, the electrolyte was believed to penetrate into composite not only from the surface of the carbon shell but also the interface of the hollow cavity inside

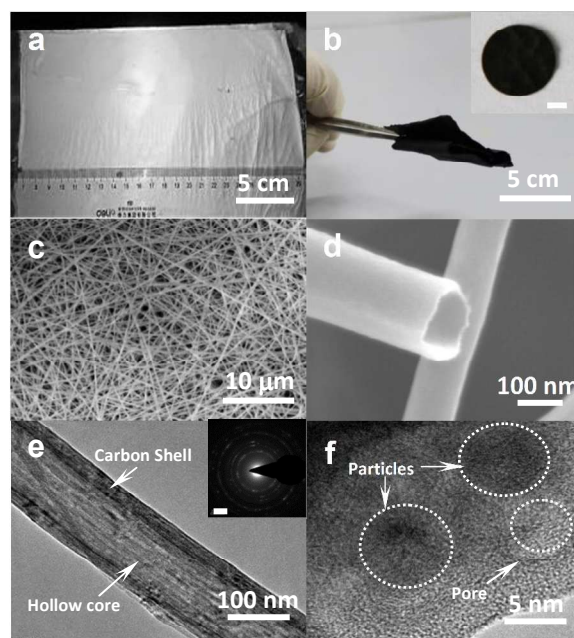


Fig. 1 The morphology of flexible TiO₂/VO₂ co-impregnated HCNFs: (a) the appearance of electrospun nanofiberous membrane; (b) self-standing nanofiberous membrane after post-annealing treatment with the electrode inset (the bar of 3 mm); (c) SEM image of membrane interface with the micrometer-scaled pores; (d) SEM image of the hollow nanofiber; (e) TEM image of the co-axial hollow architecture with the SAED pattern inset (bar of 5 1/nm); (f) HRTEM image of the carbon shell with the appearance of irregular mesopores.

The crystallographic properties of the prepared structure were further evaluated by XRD, EDS and XPS in Fig. 2. Fig. 2a illustrated the crystallinity of impregnated TiO₂ by XRD detection. The measurement with $2\theta=10-80^\circ$ indicated the

formation of anatase TiO₂, index to JCPDS No. 89-4921. Furthermore, the low-angle XRD in the region of $2\theta=0.5-1.5^\circ$ detected the broad absorption signal around $2\theta=1.1^\circ$, corresponding to the pore size of 5-10 nm, in accordance with the result of HRTEM. The EDS measurement (shown in Fig. 2a inset) verified the presence of titanium, vanadium and carbon element. The molecular ratio of carbon and titanium oxide was found to be 1:1.2. It should be pointed out that no VO₂ peak was detected, and it was possibly due to the substitution of V⁴⁺ ions with the Ti⁴⁺ ions in the TiO₂ lattice because the structures of TiO₂ and VO₂(A) are very similar. XPS spectrums with narrow energy bonding region of Ti2p and V2p were further proposed, indicating the valence of titanium and vanadium element of co-impregnated TiO₂/VO₂ in the carbon shell. In Fig. 2b and c, typical Ti (IV) bonding energy at 458.4/ 464.0 eV and V (IV) at 517.1/523.2 eV was detected, firmly proving that TiO₂ and VO₂ that has been successfully loaded into the carbon shell.^{19, 20}

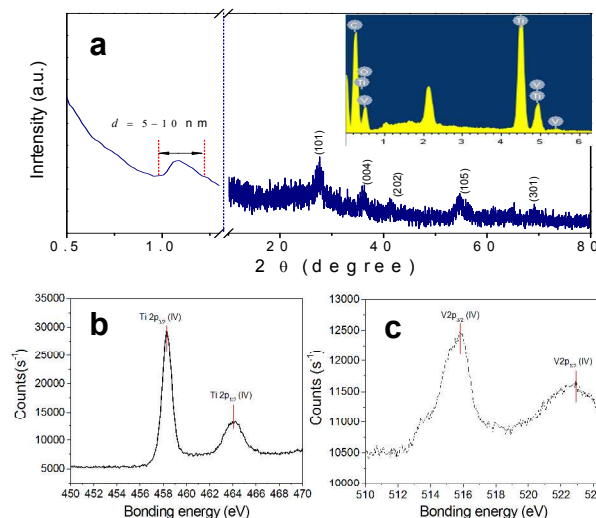


Fig. 2 Crystallographic characterization of TiO₂/VO₂ co-impregnated HCNFs: (a) the XRD and low-angle XRD spectrum with the EDS spectrum inset; (b) the XPS spectrum of narrow bonding energy region of Ti2p; (c) the XPS spectrum of narrow bonding energy region of V2p.

In order to investigate the lithiation/delithiation process of the unique structure, CV test was carried out and results were shown in Fig. 3. A pair of broad redox peaks (in Fig. 3a) were recognized as the Ti(IV)/Ti(III) with the anodic and cathodic peaks located at 2.0 V/1.5 V (vs. Li⁺/Li). When the scan rate consequently increased from 0.3 to 2.0 mV s⁻¹, slight shift of the anodic/ cathodic peak location occurred due to the limited kinetics of lithium ion insertion. In this case, unlike other active materials with sharp and narrow redox peaks, TiO₂ and VO₂ exhibited relatively broad ones. The reason has been explained in literature that TiO₂/VO₂ has both intercalation and capacitance properties with lithium ions.²¹⁻²⁷ As a result, lithium ion inserting into the lattice or adsorbing on the surface can both contribute to the sum of charge delivered. It was obvious that although TiO₂ and VO₂ particles were embedded in carbon, the redox reaction maintained, suggesting the exceptional porous carbon structure that has enabled the fast electron transfer and electrolyte penetration. Furthermore, we tried to quantitatively distinguish the capacitance from the intercalation capacity (Eqn. S1†).²⁸ As suggested by Fig. 3b, the surface capacitance was believed to contribute 41%, 64% and 67% of the total charge under the scan rate of 0.3, 0.5 and 0.8 mV s⁻¹, respectively. And the detailed contribution ratio of capacitance and intercalation capacity for each

scan rate was listed in Fig. S1†. The results revealed that with fast scan rate (0.8 mV.s⁻¹), capacitance behavior played more important role than that of intercalation capacity. The capacitance behavior may ensure an improvement of high power rate.

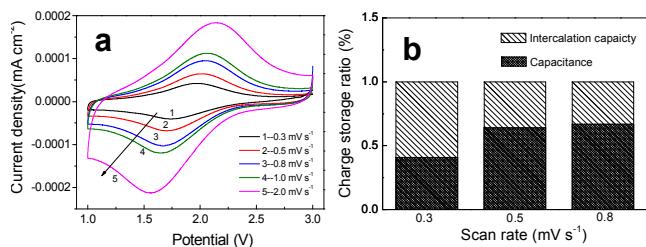


Figure 3 CV investigation of TiO₂/VO₂ co-encapsulated HCNFs: (a) redox behavior in the potential range of 1-3 V with different scan rate; (b) the proportion of intercalation capacity and capacitance under scan rate of 0.3, 0.5 and 0.8 mV s⁻¹.

Benefitting from the unique structure, ultra-fast rate performance and long-term stability under high rate were measured by the galvanostatic experiment within the potential range of 0-3 V and 1-3 V (vs. Li⁺/Li) in Fig. 4. In term of 0-3 V potential range, the anode capacity was found to be 1058, 849, 576, 440, 338, 248, 210 and 160 mAh g⁻¹ under the current density of 0.3 C, 1 C, 2 C, 5 C, 7 C, 10 C, 15 C and 20 C (1 C=335 mA g⁻¹) (Fig. S2†). The ultra-high capacity is considered to be not only from the TiO₂/VO₂ but also from the HCNFs, because CNFs itself can deliver capacity within 0-1 V due to the lithium ion insertion into carbon layers. According to Liu's research, narrowing the potential range to 1-3 V can exclude the possible capacity from CNFs.¹⁸ Therefore, the real capacity delivered by TiO₂/VO₂ impregnated in the unique structure was re-evaluated and illustrated in Fig. 4a. Capacity of 516, 468, 407, 301, 241, 215, 180 and 101 mAh g⁻¹ was obtained, still higher than current reported ones. Additional 50 cycles under 0.3 C current density was consequently conducted, suggesting a good retention ability of the unique structure. Furthermore, cycling performance at very high current density (15 C and 20 C) was illustrated by Fig. 4b. Stable cycling ability was illustrated with 92 % and 87 % capacity retention after 1000 cycles within 1-3 V. The corresponding charge/discharge profile of rate performance was shown in Fig. 4c. The plateau of delithiation at 2.0 V and the plateau of lithiation at 1.5 V were observed. However, the plateau was not critically flat largely due to the capacitor-like lithiation/delithiation behavior, suggested by the CV test. Most importantly, the problem of low coulombic efficiency that has severely limited the application of transition metal oxide has been improved by the unique structure. The coulombic efficiency of the first and second cycles was 99.2 % and 100.6 % and it maintained about 100 % for the following cycles. The initial discharge process from open circuit voltage to 1.0 V can be seen in Fig. S3†. Meantime, it is reported that small amount of vanadium oxide would significantly improve the cycling performance of TiO₂.²⁹ Therefore, the co-impregnation of TiO₂ with VO₂ is believed contributed to the ultra-long lifespan of the cell.

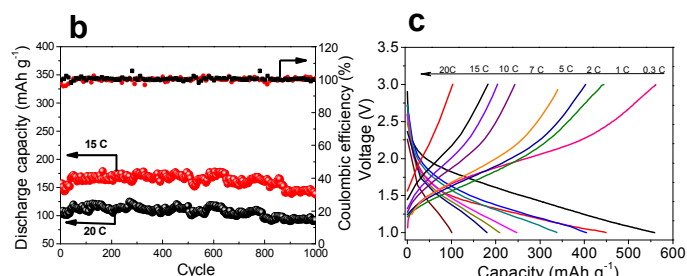
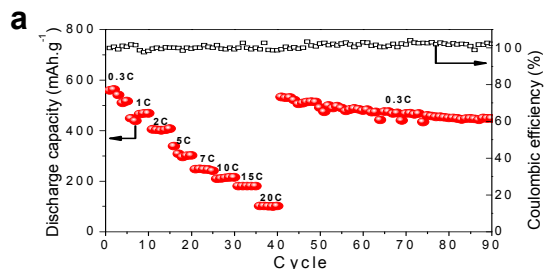


Figure 4 Battery performance of TiO₂/VO₂ co-impregnated HCNFs: (a) high power rate performance and good retention ability from 0.3 C to 20 C; (b) cycling performance under 15 C and 20 C; (c) corresponding charge/discharge profiles of rate performance.

We next evaluated the electrochemical properties of TiO₂/VO₂ co-impregnated HCNFs by electrochemical impedance spectrum (EIS) measurements shown in Fig. 5. In Fig. 5a a comparison of EIS spectra was made regarding cells with different potential ranges after rate performance test. It is revealed that the EIS of cell with 0-3V appeared to be two semicircles whereas that with 1-3V only showed one obvious semicircle. The difference indicated the formation of SEI membrane on the surface of HCNFs. In order to determine the Warburg coefficient (σ_w) of the unique structure, the plots of Z_{re} vs. $\omega^{-0.5}$ was depicted with perfect fitting in Fig. 5b. The electrochemical properties of the resistance of electrolyte (R_e), the resistance of electrochemical reaction (R_{ct}), the diffusion coefficient (D) as well as exchange current density (i_0) has been thus determined by Eqn. S2, S3 and S4† and summarized in Table 1. In term of the cell operated at 1-3 V, the R_{ct} of the unique structure has been intensively lowered to 66 Ω , compared to that of the pure TiO₂ about $\sim 400 \Omega$. It suggested a very good contact between the TiO₂/VO₂ particles with the HCNFs. Most importantly, the diffusion of lithium ion in the active material has been extremely improved. Wang *et al.* investigated the kinetics of TiO₂ single crystal and proposed the diffusion coefficient to be $1.3 \times 10^{-13} \text{ cm}^2 \text{ S}^{-1}$.³⁰ In this study, when HCNFs was utilized as the immobilizer for TiO₂/VO₂ particles impregnation, the diffusion coefficient increased to $9.25 \times 10^{-10} \text{ cm}^2 \text{ S}^{-1}$ with the exchange current density of $3.88 \times 10^{-4} \text{ A cm}^{-2}$, which suggesting the a more advantageous environment for fast electrolyte penetration. In term of cell operated at 0-3 V, the formation of SEI membrane has shown negative effect on the lithium ion diffusion and insertion efficiency.

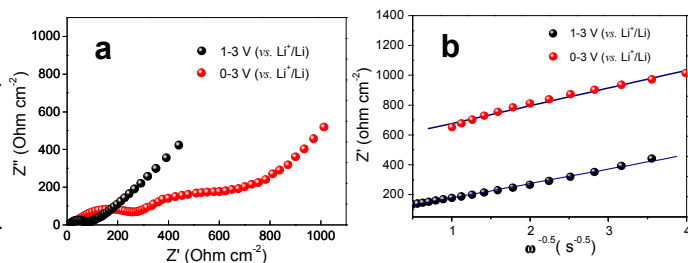


Table 1 Electrochemical properties of TiO₂/VO₂ co-impregnated HCNFs with different potential window

Potential/V	R_e/Ω	R_{ct}/Ω	R_{ESI}/Ω	R_{sum}/Ω (fitted) ^{a)}	$D/\text{cm}^2 \text{ s}^{-1}$	$i_0/\text{A cm}^{-2}$
1-3	13.11	66.16	None	80.25	9.25×10^{-10}	3.88×10^{-4}
0-3	23.68	255.1	275.3	557.5	4.98×10^{-11}	1.01×10^{-4}

a) The value of R_{sum} (including R_e , R_{ct} and R_{ESI}) was calculated from $Z''-\omega^{-0.5}$ plot

Conclusions

In summary, we rationally designed a flexible nanofibrous anode for high performance LIBs by co-encapsulating TiO₂ and VO₂ nanoparticles into hollow carbon nanofibers. In-situ growth of TiO₂ and VO₂ exhibited exceptional contact with carbon shell, which largely improved the conductivity. The hierarchical porous structure of the unique HCNFs formed a continuous 3D electronic path, facilitated fast electrolyte penetration and sufficient lithium ion insertion. As a result, good conductivity, highly reversible capacity, excellent rate performance and ultra-long cycling stability were obtained and the structure was considered as an exceptional improvement on the design of TiO₂/carbon nanostructured composite. This rational structural design may provide a facile route for the fabrication of metal-oxide/Carbon composite electrodes with high capacity and good stability.

Acknowledgements

The authors gratefully acknowledge the financial support from the Major State Basic Research Development Program of China (973 program) under grant No. 2013CB632601, National Natural Science Foundation of China under Grant Nos. 51274178 and 51274179 and the financial support from the China Scholarship Council (CSC).

Notes and references

^aNational Engineering Laboratory for Hydrometallurgical Cleaner Production Technology, Key Laboratory of Green Process and Engineering, Institute of Process Engineering, Chinese Academy of Sciences, Beijing, China.

^bUniversity of Chinese Academy of Sciences, No.19A Yuquan Road, Beijing, China.

*Corresponding author: Hao Du, Fax: 86 10 82544856; Tel: 86 10 82544856; E-mail: duhao121@hotmail.com

Electronic Supplementary Information (ESI) available: [details of any supplementary information available should be included here]. See DOI: 10.1039/b000000x/

- K. Kang, Y. S. Meng, J. Bréger, C. P. Grey and G. Ceder, *Science*, 2006, **311**, 977-980.
- J. M. A. M. Tarascon, *Nature*, 2001, **414**, 359.
- P. G. Bruce, B. Scrosati and J.-M. Tarascon, *Nanomaterialien für wiederaufladbare Lithiumbatterien*, 2008, 2930.
- K. Kang, Y. S. Meng, J. Bréger, C. P. Grey and G. Ceder, *Science*, 2006, 977.
- R. Akolkar, *JOURNAL OF POWER SOURCES*, **232**, 23-28.
- K. S. Park, S. G. Doo, A. Benayad and D. J. Kang, *Journal of the American Chemical Society*, 2008, **130**, 14930-14931.
- G. N. Zhu, Y. G. Wang and Y. Y. Xia, *ENERGY AND ENVIRONMENTAL SCIENCE*, 2012, **5**, 6652-6667.
- A. R. Armstrong, G. Armstrong, J. Canales, R. García and P. G. Bruce, *Advanced Materials*, 2005, **17**, 862-865.
- A. R. Armstrong, V. Gentili, P. G. Bruce, C. Arrouvel, S. C. Parker and M. S. Islam, *Chemistry of Materials*, 2010, **22**, 6426-6432.
- J. S. Chen and X. W. Lou, *Electrochemistry Communications*, 2009, **11**, 2332-2335.
- J. Y. Shin, D. Samuelis and J. Maier, *Advanced Functional Materials*, 2011, **21**, 3464-3472.
- B. Rambabu, V. Subramanian, A. Karki, K. I. Gnanasekar and F. P. Eddy, *Journal of Power Sources*, 2006, **159**, 186-192.
- J. Wang, Y. Bai, M. Wu, J. Yin and W. F. Zhang, *Journal of Power Sources*, 2009, **191**, 614-618.
- C. Lai, Z. Zhou, L. Zhang, X. Wang, Q. Zhou, Y. Zhao, Y. Wang, X.-F. Wu, Z. Zhu and H. Fong, *Journal of Power Sources*, 2014, **247**, 134-141.
- M. N. Hyder, S. W. Lee, F. C. Cebeci, D. J. Schmidt, Y. Shao-Horn and P. T. Hammond, *Acs Nano*, 2011, **5**, 8552-8561.
- C. Kim, K. S. Yang, M. Kojima, K. Yoshida, Y. J. Kim, Y. A. Kim and M. Endo, *Advanced Functional Materials*, 2006, **16**, 2393-2397.
- Q. Si, K. Hanai, T. Ichikawa, M. B. Phillipps, A. Hirano, N. Imanishi, O. Yamamoto and Y. Takeda, *Journal of Power Sources*, 2011, **196**, 9774-9779.
- S. Liu, Z. Wang, C. Yu, H. B. Wu, G. Wang, Q. Dong, J. Qiu, A. Eychmueller and X. W. Lou, *Advanced Materials*, 2013, **25**, 3462-3467.
- A. A. Galuska, J. C. Uht and N. Marquez, *J. VACUUM SCI. & TECHNOL. A*, 1988, **6**, 110-122.
- M. C. Biesinger, L. W. M. Lau, A. R. Gerson and R. S. C. Smart, *Applied Surface Science*, 2010, **257**, 887-898.
- P. G. Bruce, B. Scrosati and J. M. Tarascon, *Angewandte Chemie-International Edition*, 2008, **47**, 2930-2946.
- D. V. Bavykin, J. M. Friedrich and F. C. Walsh, *Advanced Materials*, 2006, **18**, 2807-2824.
- Y. G. Guo, J. S. Hu and L. J. Wan, *Advanced Materials*, 2008, **20**, 2878-2887.
- Q. Wang, Z. H. Wen and J. H. Li, *Advanced Functional Materials*, 2006, **16**, 2141-2146.
- H. B. Zhao, L. Y. Pan, S. Y. Xing, J. Luo and J. Q. Xu, *Journal of Power Sources*, 2013, **222**, 21-31.
- J. F. Liu, Q. H. Li, T. H. Wang, D. P. Yu and Y. D. Li, *Angewandte Chemie-International Edition*, 2004, **43**, 5048-5052.
- M. D. Wei, H. Sugihara, I. Honma, M. Ichihara and H. S. Zhou, *Advanced Materials*, 2005, **17**, 2964-+.
- J. Wang, J. Polleux, J. Lim and B. Dunn, *Journal of Physical Chemistry C*, 2007, **111**, 14925-14931.
- A. Ly Tuan, A. K. Rai, T. Trang Vu, J. Gim, S. Kim, E.-C. Shin, J.-S. Lee and J. Kim, *Journal of Power Sources*, 2013, **243**, 891-898.
- J. Wang, J. Polleux, J. Lim and B. Dunn, *Journal of Physical Chemistry C*, 2007, **111**, 14925-14931.

High anodic power rate and ultra-long cycling stability were achieved by co-encapsulation of TiO_2/VO_2 into hollow carbon nanofibers.

